

Scale-hopping approaches in designing complex alloys

J. Millan, D. Ponge, I. Pvstugar, S. Sandlöbes, P. Choi, S. Zaefferer, S.M. Hafez Haghighat, G. Eggeler, A. Nematollahi, M. Herbig, R. Kirchheim, G. Inden, J. Neugebauer, D. Raabe

WWW.MPIE.DE

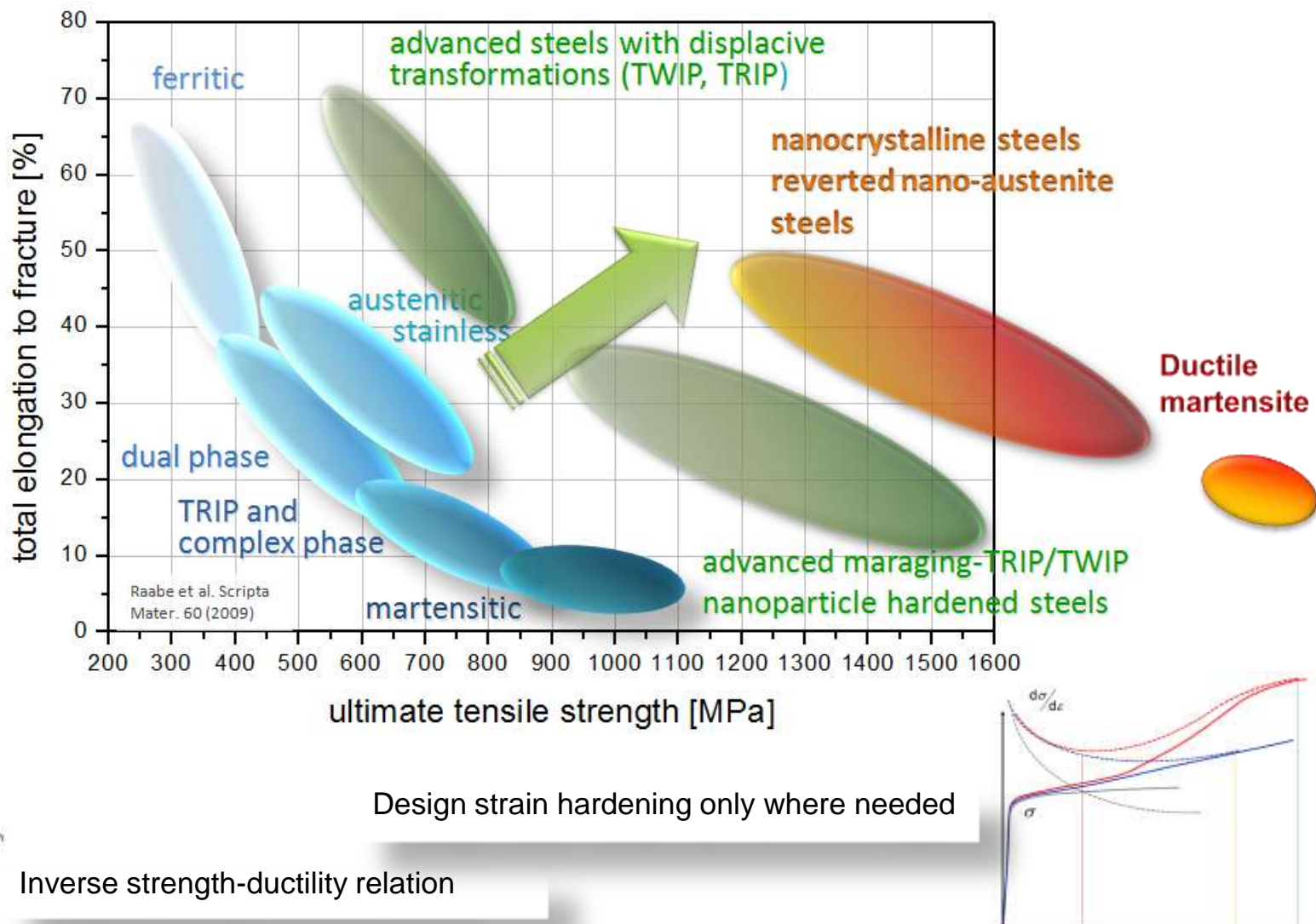
d.raabe@mpie.de



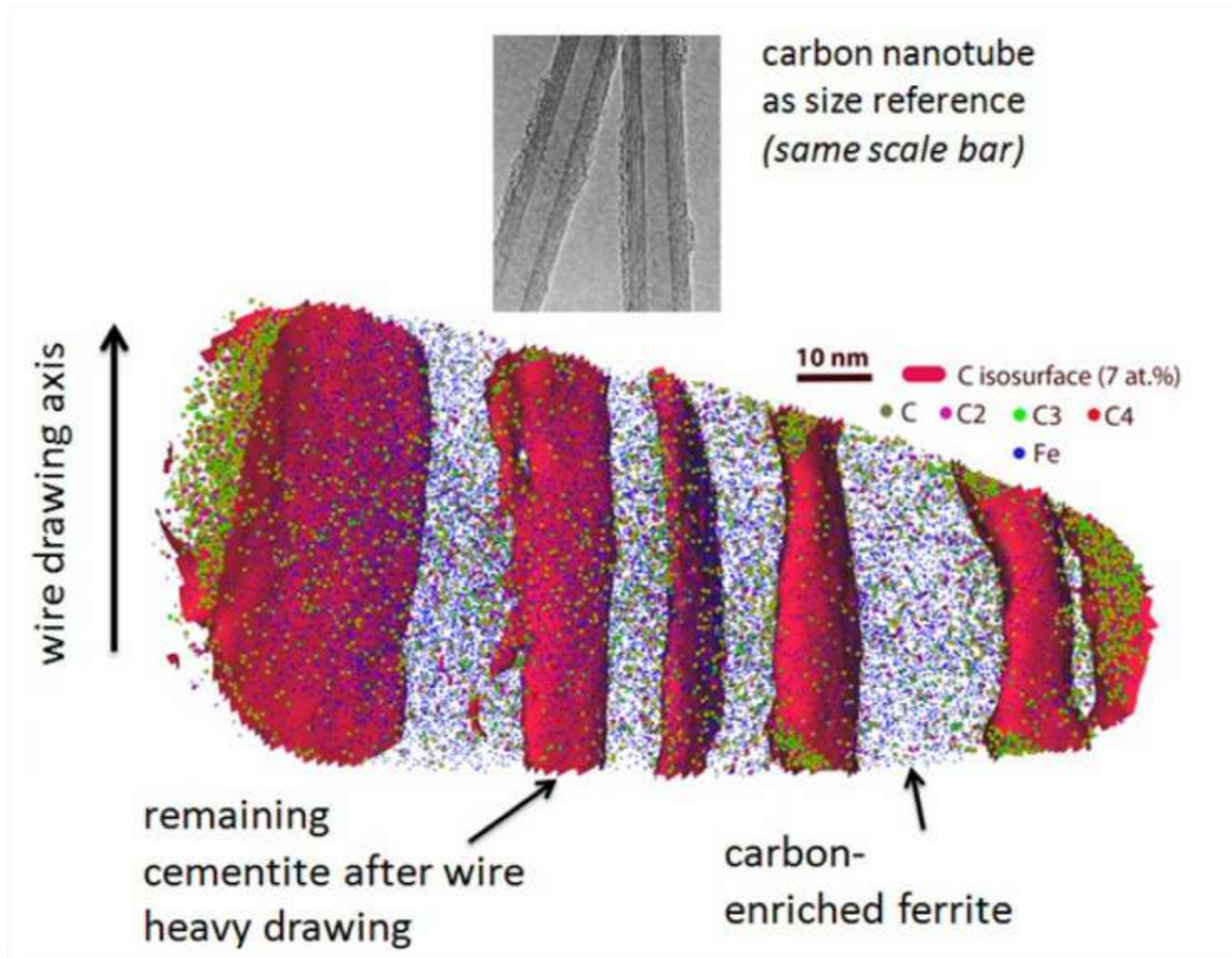
**Max-Planck-Institut
für Eisenforschung GmbH
Düsseldorf, Germany**

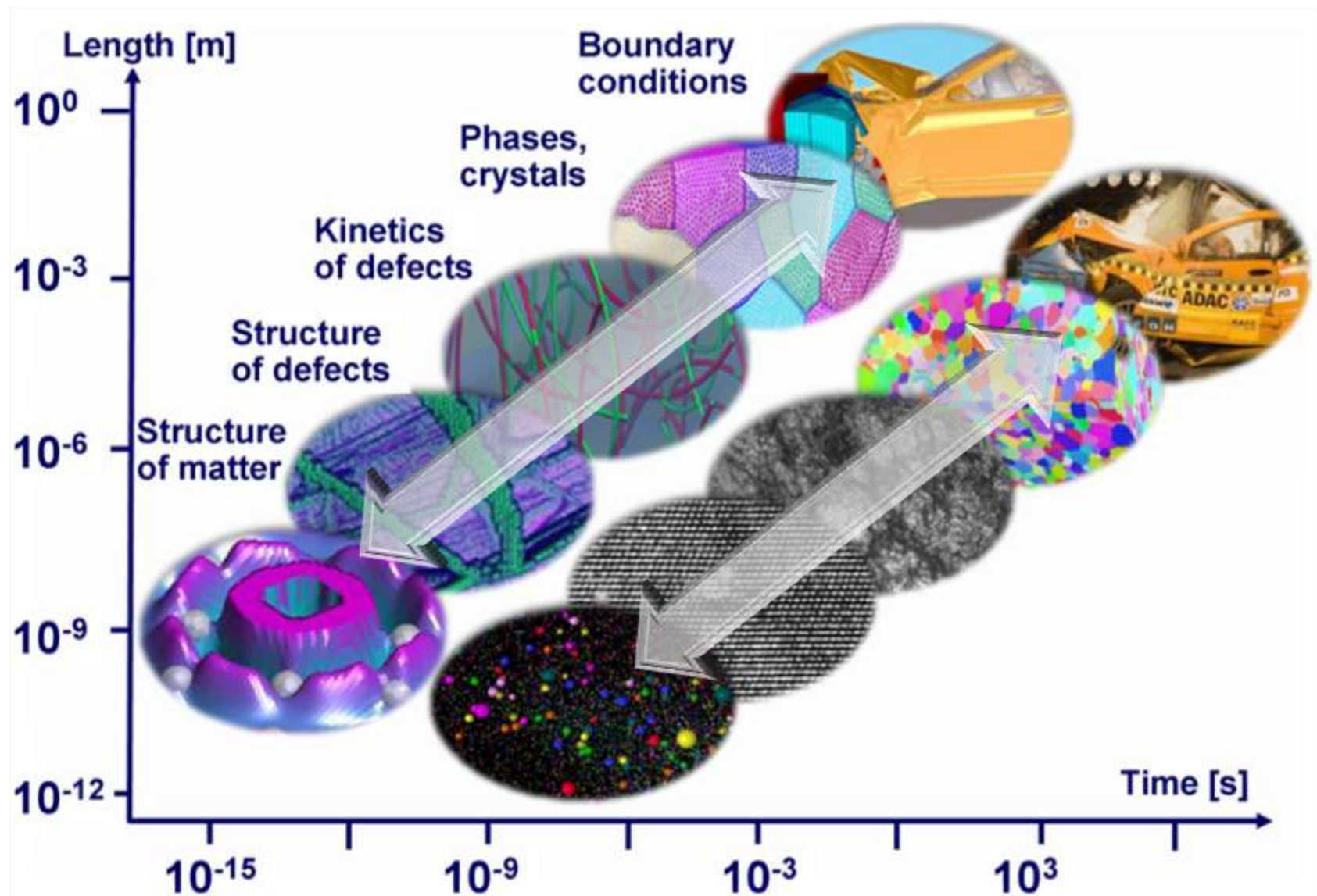
shortened version

Local phase transformations enable high strength of bulk metals

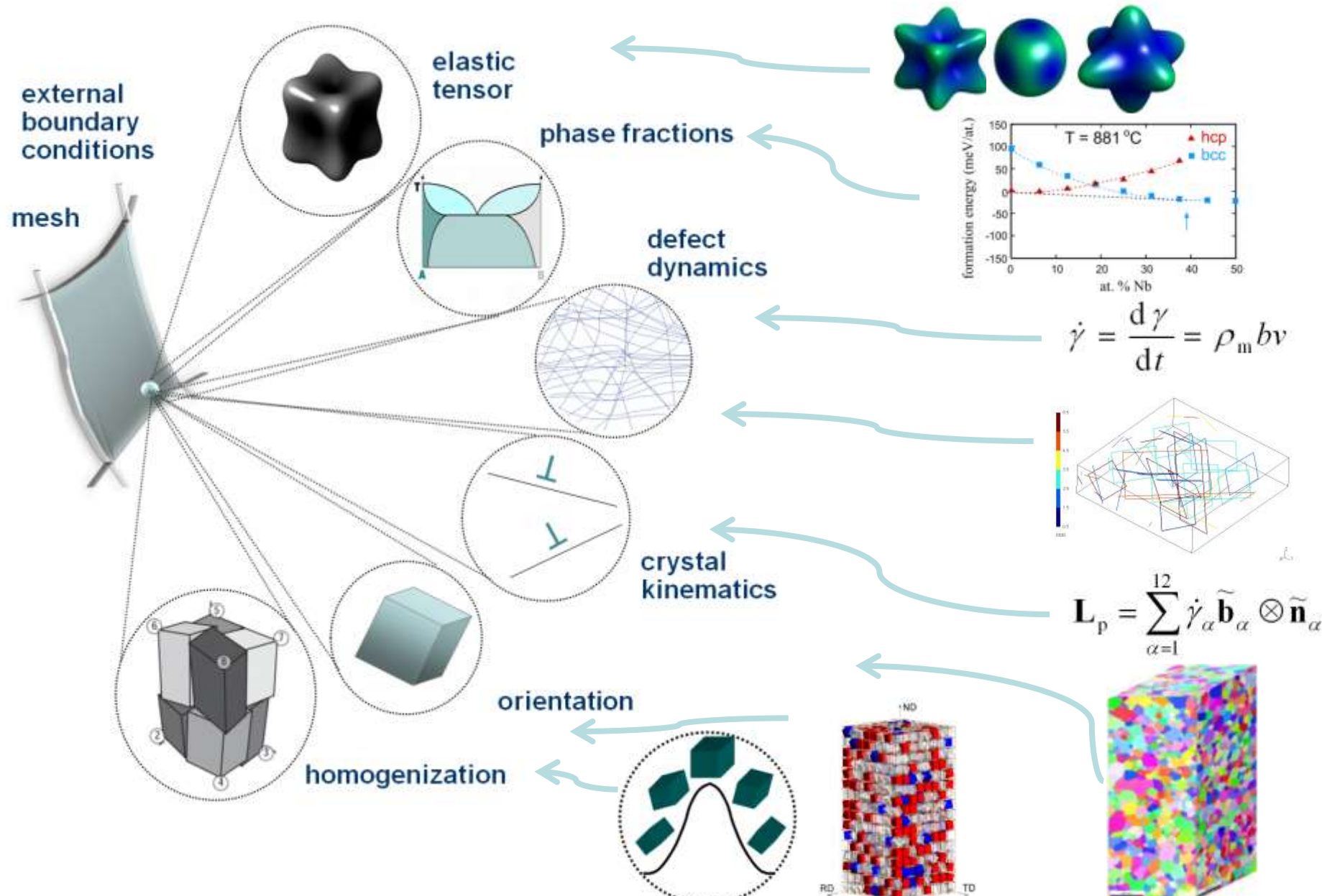


Understanding the nanoscopic length scales and their effects





Multiscale crystal plasticity FEM



Pearlite and Fe-Mn-C TWIP steels

Nano-austenite reversion

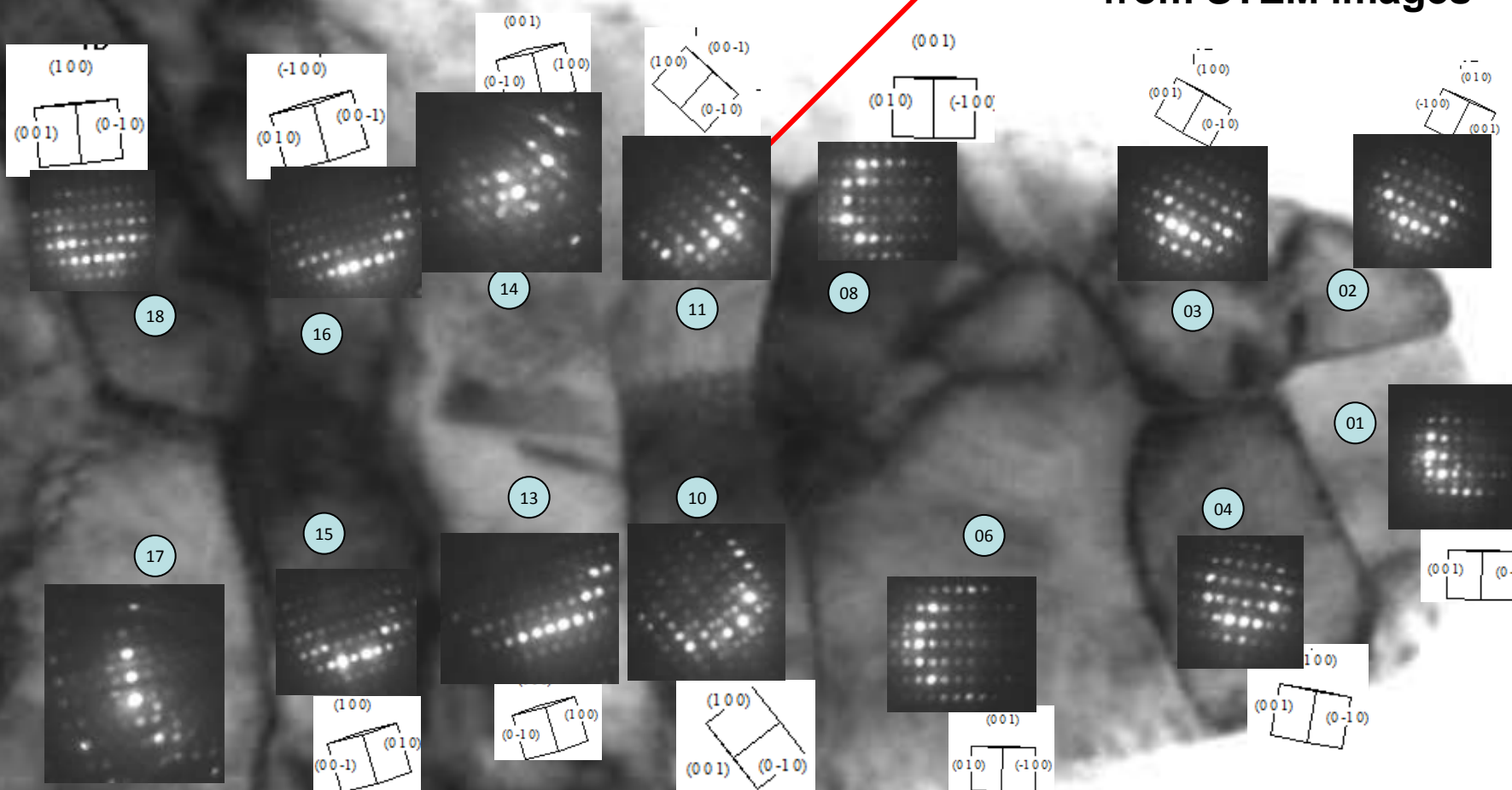
Fe-based ‘superalloy’

Superalloys

Characterization of GB segregation by correlative TEM / APT

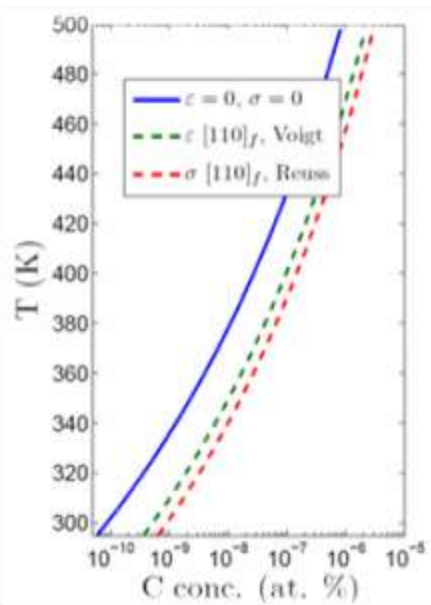
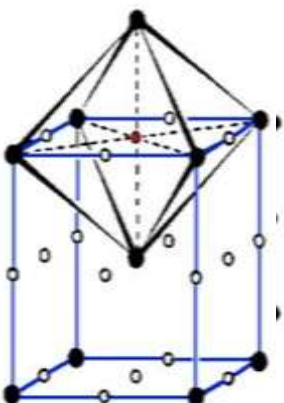


Grain boundary plane normals analyzed from STEM images

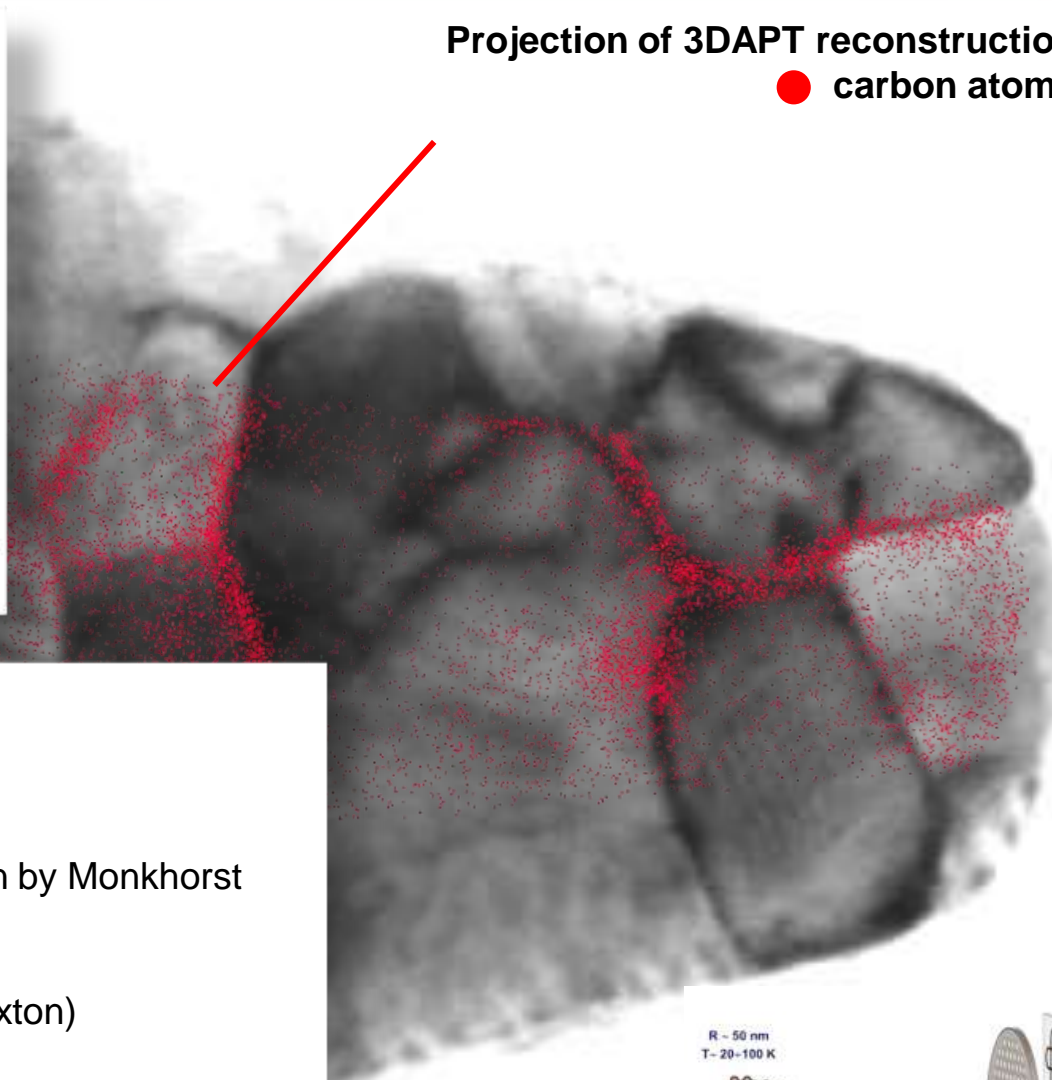


Grain orientations measured by nano beam diffraction

Characterization of GB segregation by correlative TEM / APT



Projection of 3DAPT reconstruction
● carbon atoms



Spin-polarized DFT

Projector-augmented wave method

Plane-wave basis set

Generalized-gradient-approximation (GGA)

k-point meshes for the Brillouin zone integration by Monkhorst

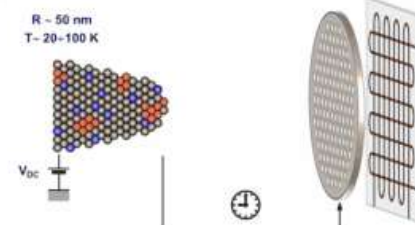
11,000 k-points (f), 20,000 k-points (c)

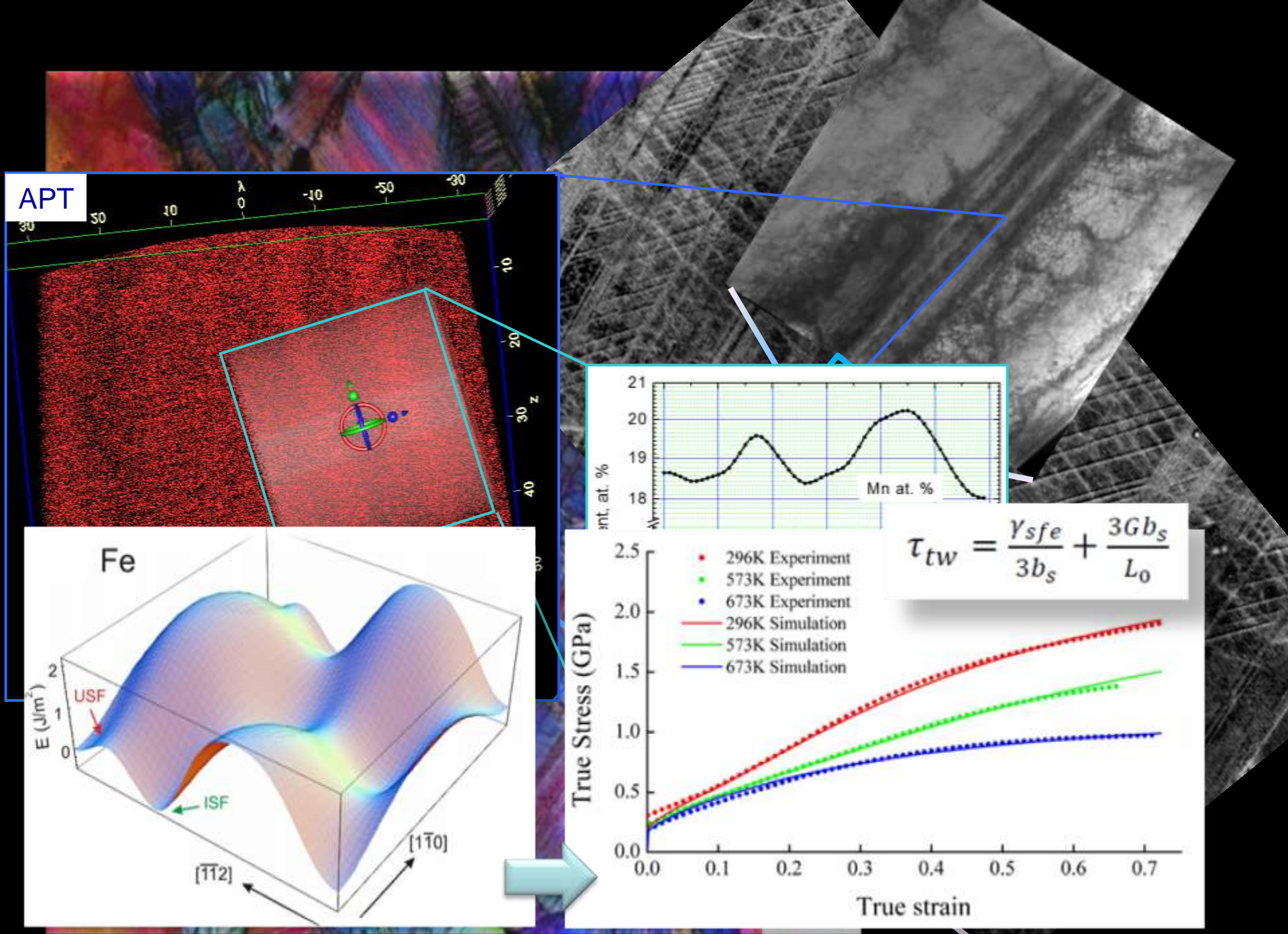
Plane-wave energy cut-off of: 450 eV

Electronic temperature: 0.2 eV (Methfessel–Paxton)

Ideal solution for entropy

Carbon grain boundary
excess measured by APT



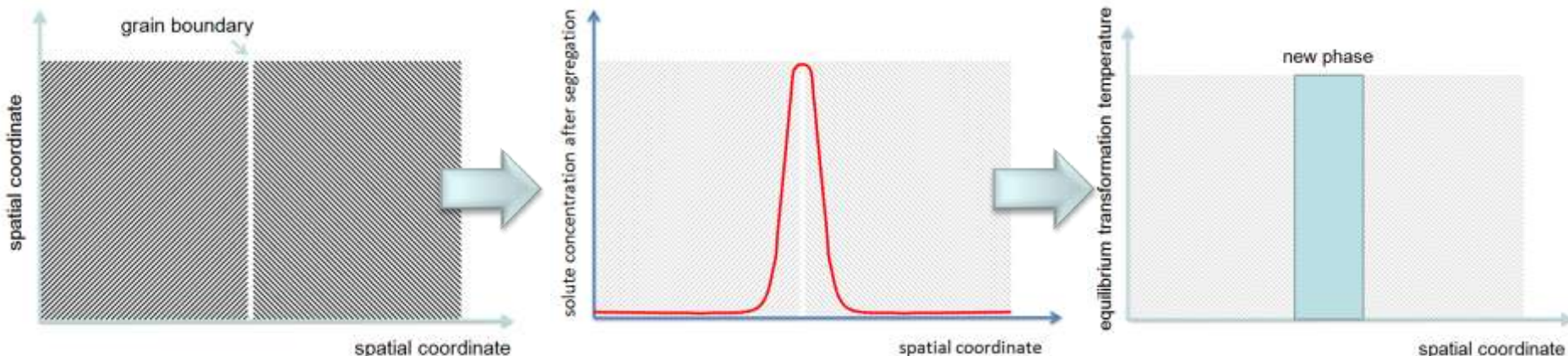


Pearlite and Fe-Mn-C TWIP steels

Nano-austenite reversion

Fe-based ‘superalloy’

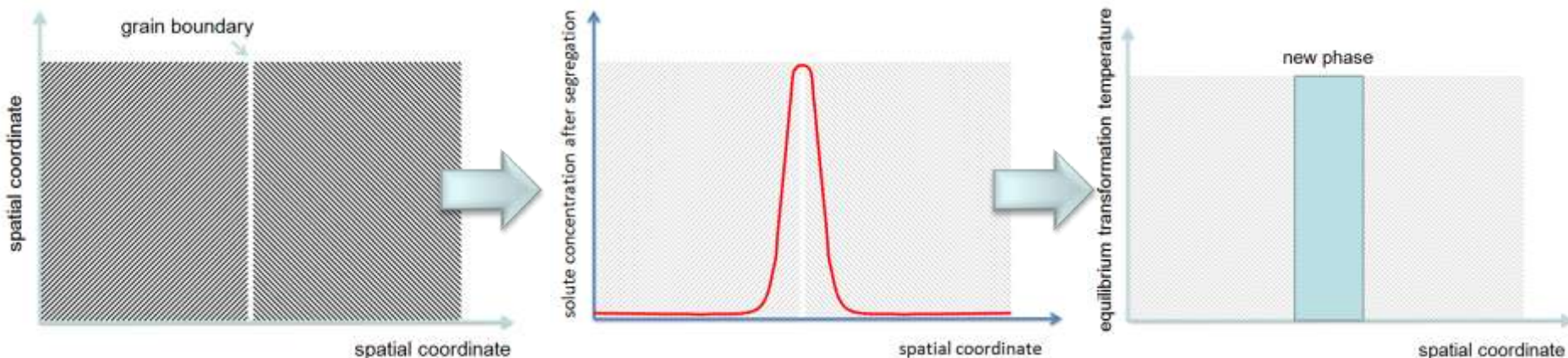
Superalloys



Solute segregation to martensite grain boundaries



Local phase transformation at grain boundary
(martensite-to-austenite reversion confined to GB)

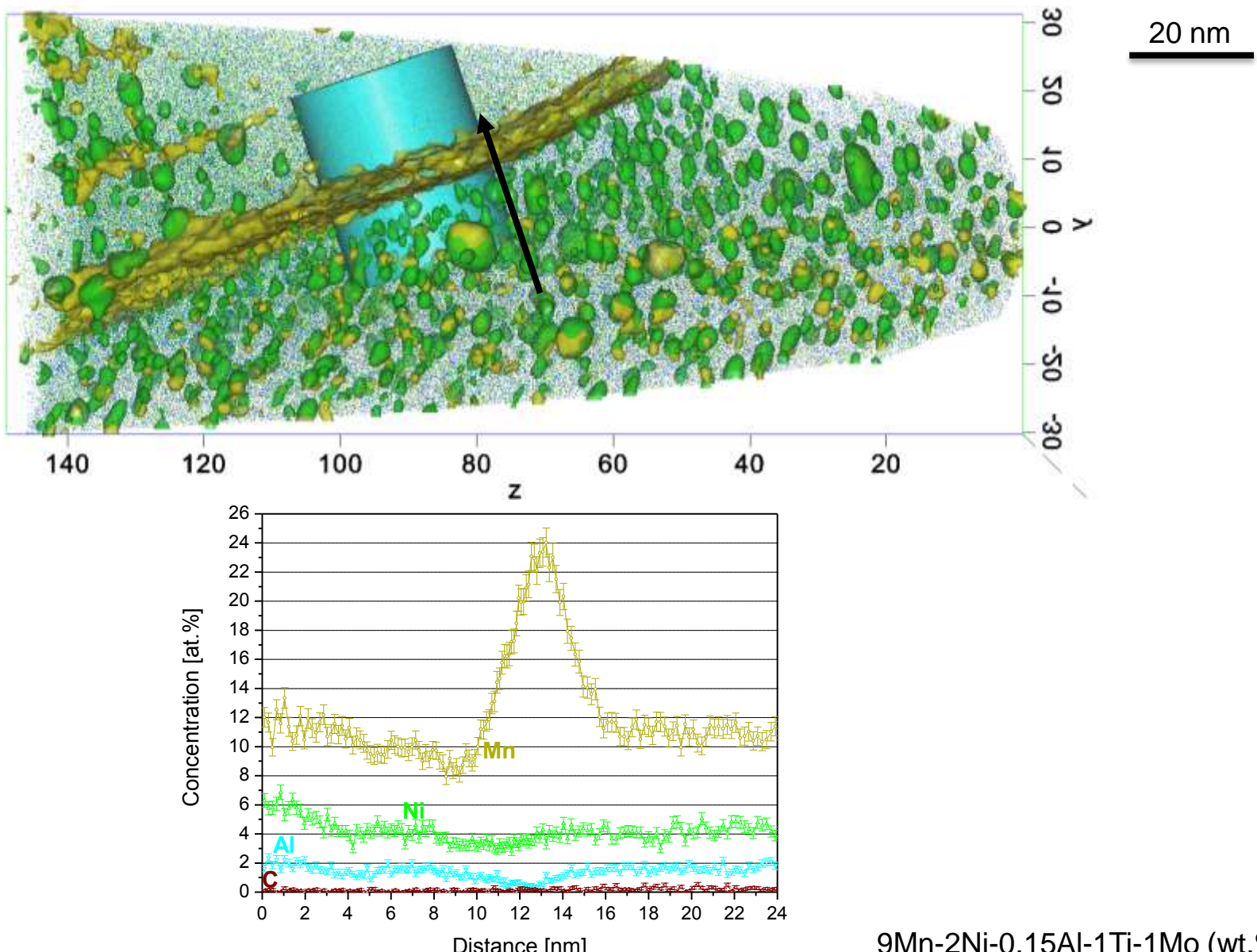


Solute segregation to martensite grain boundaries

- Element with high segregation tendency
- Reduce transformation temperature (e.g. from martensite to austenite)
- Prefer segregation over bulk precipitation (e.g. carbide)

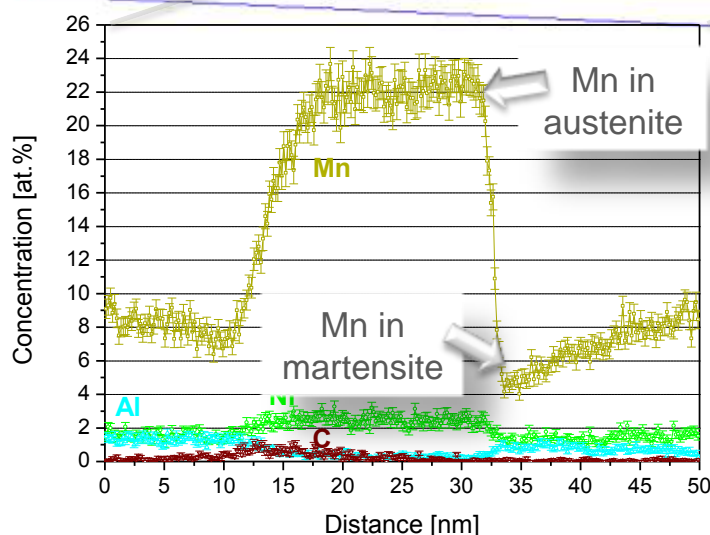
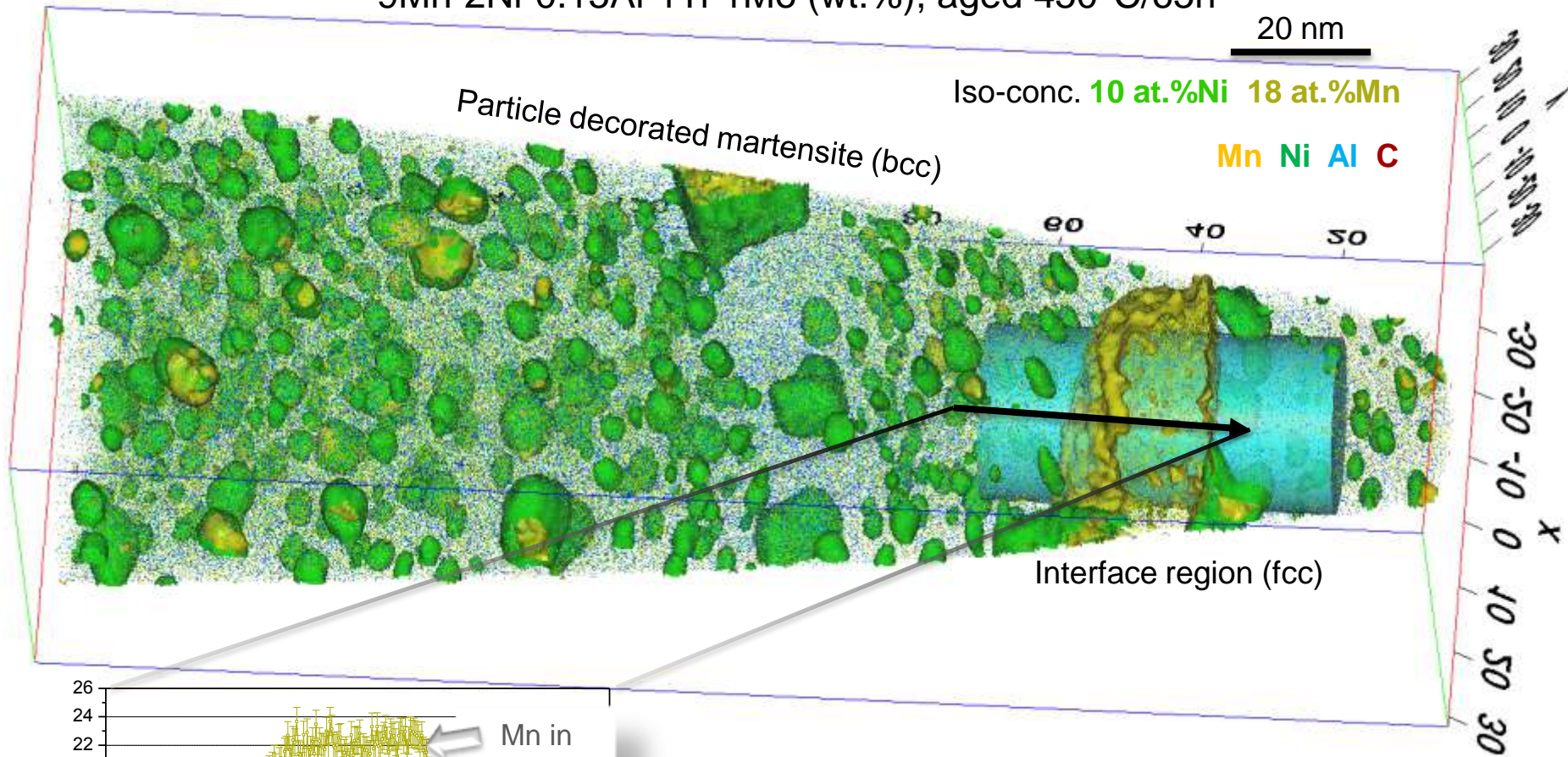
Local phase transformation at grain boundary
(martensite-to-austenite reversion confined to GB)

Mn segregation at grain boundary, (450°C/65h)

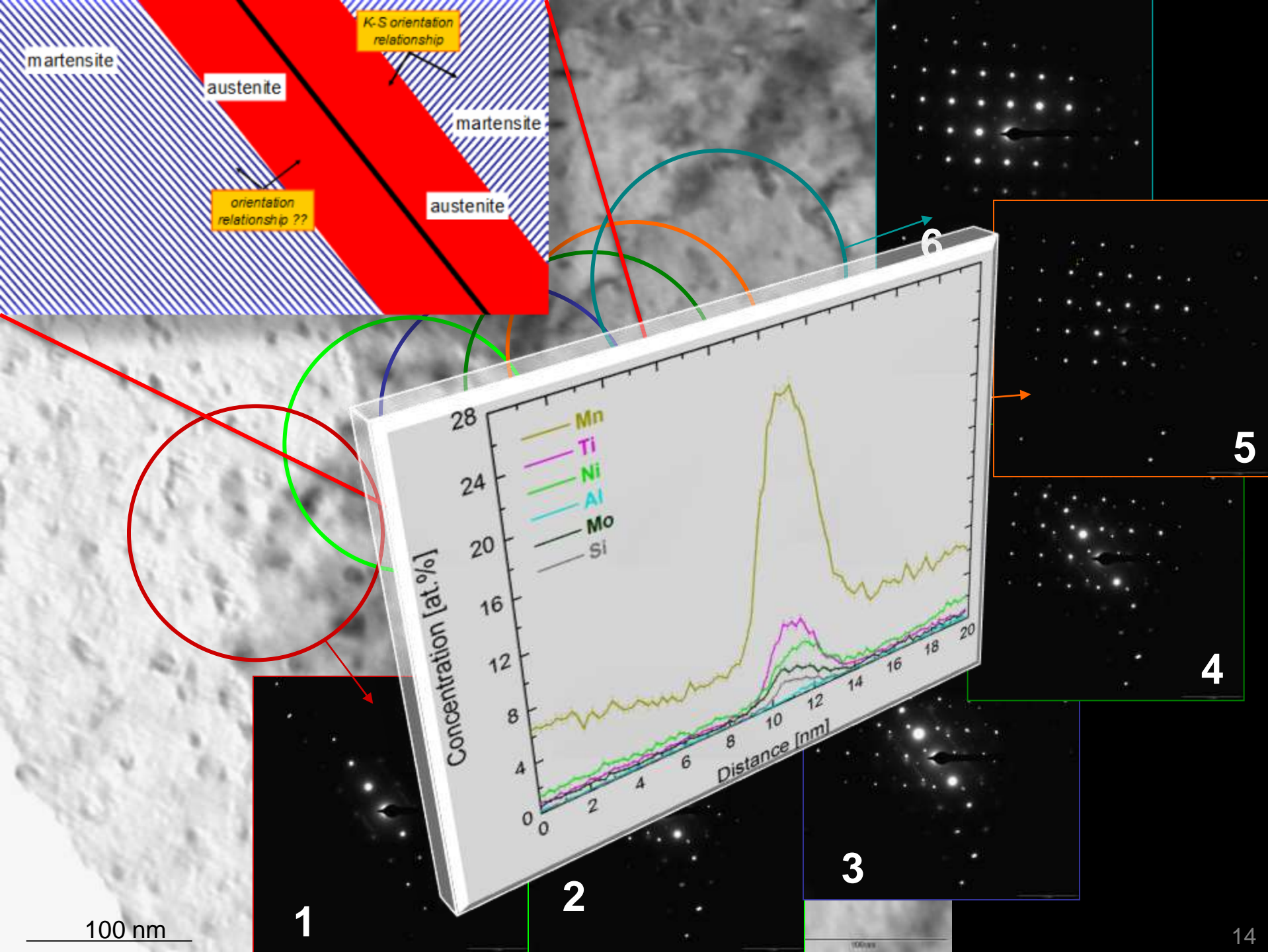


9Mn-2Ni-0.15Al-1Ti-1Mo (wt. %)

20 nm



Phase formation at martensite interface
Near-equilibrium partitioning at interface



Pearlite and Fe-Mn-C TWIP steels

Nano-austenite reversion

Fe-based ‘superalloy’

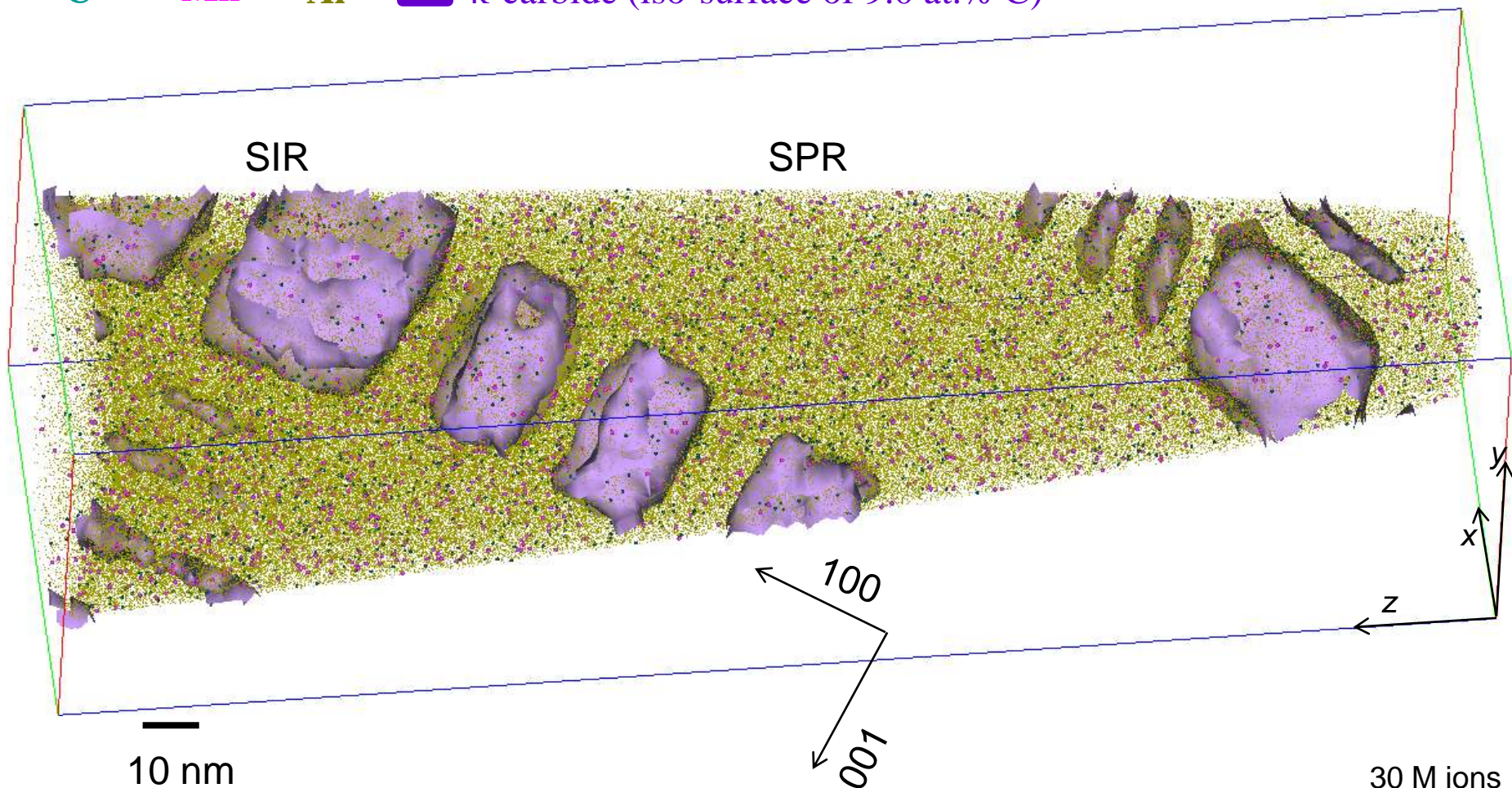
Superalloys

Growth of κ -carbides



Aged for **168 h** at 600°C

● C ● Mn ● Al ■ κ -carbide (iso-surface of 9.0 at.% C)



Pearlite and Fe-Mn-C TWIP steels

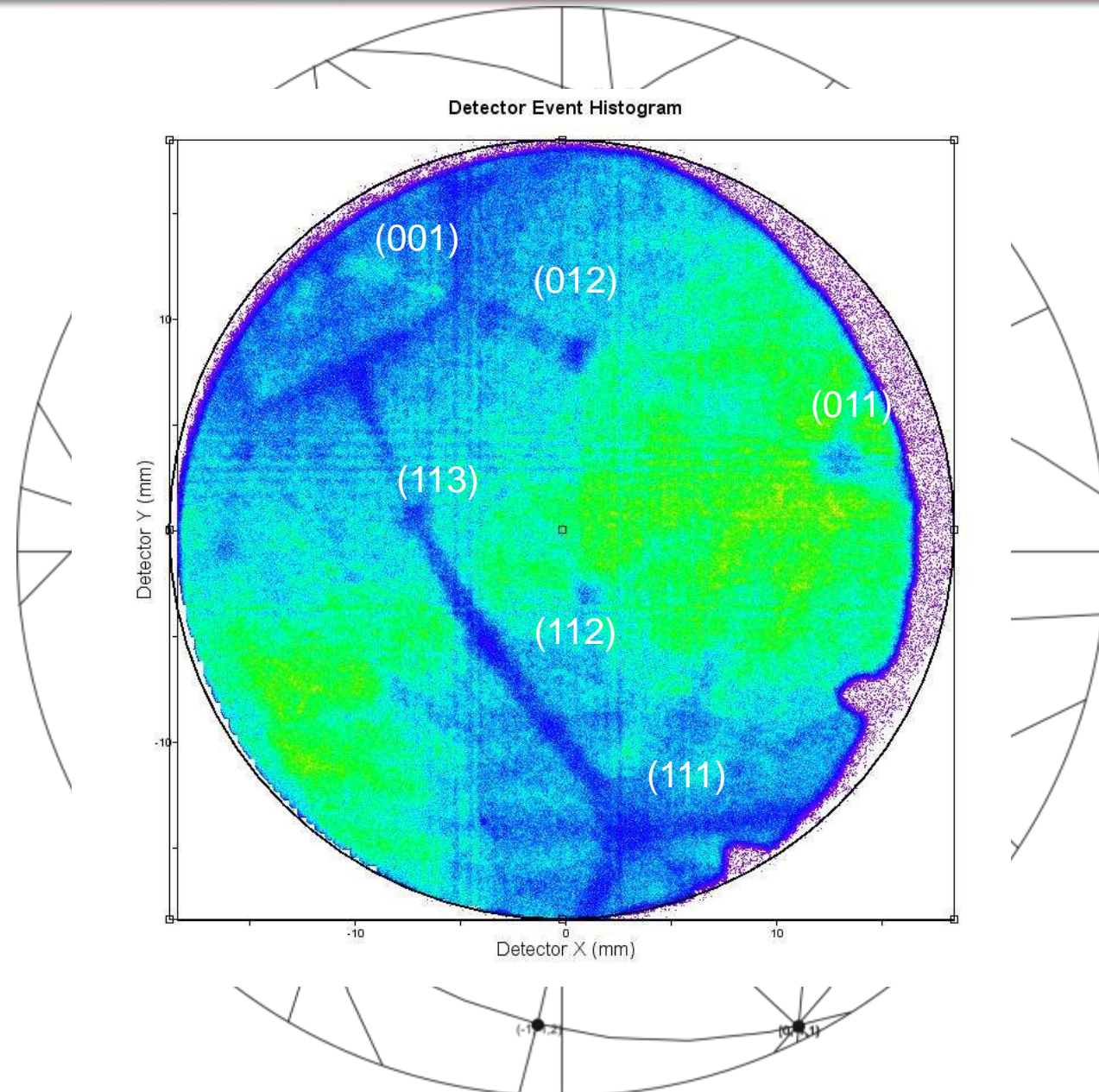
Nano-austenite reversion

Fe-based ‘superalloy’

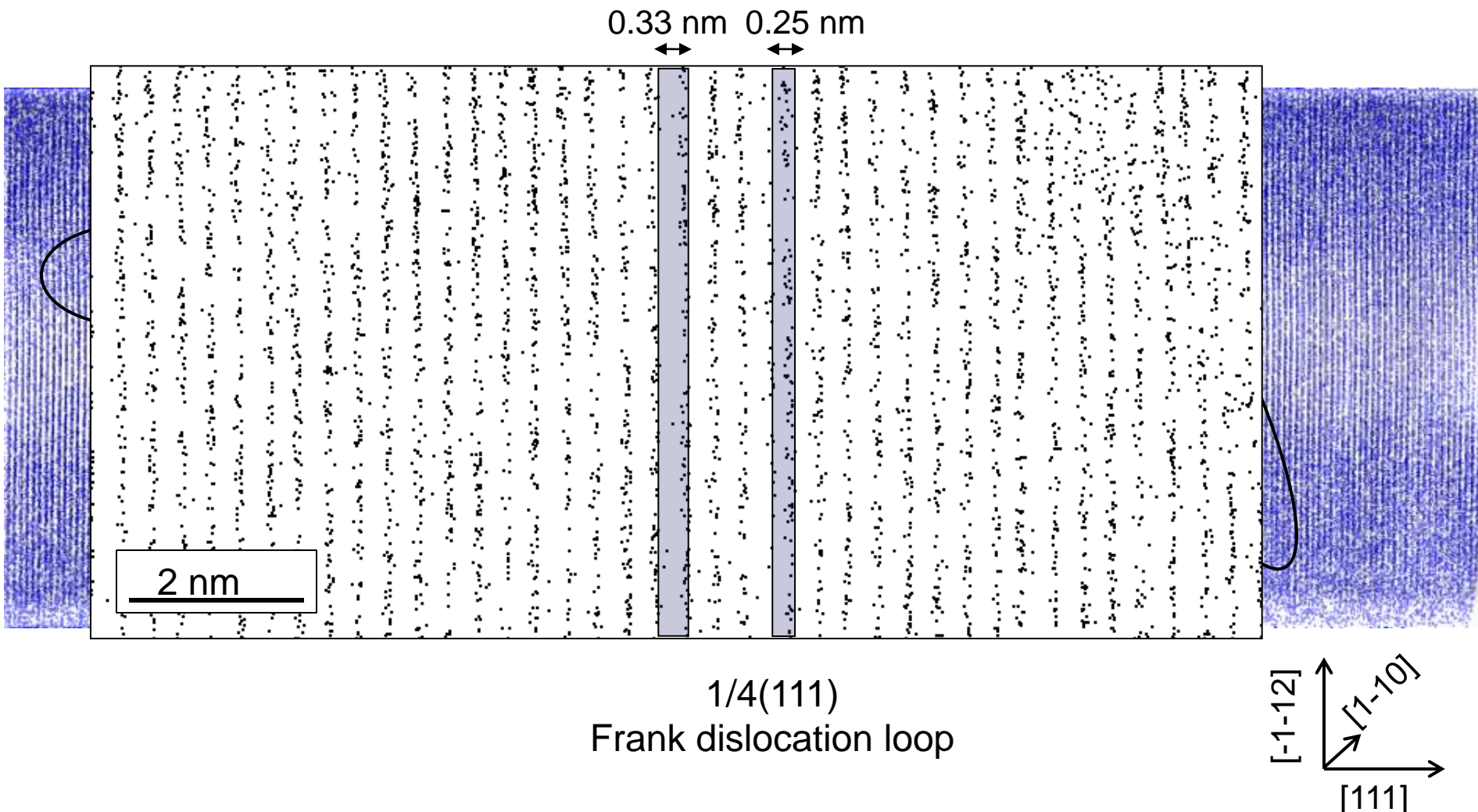
Superalloys



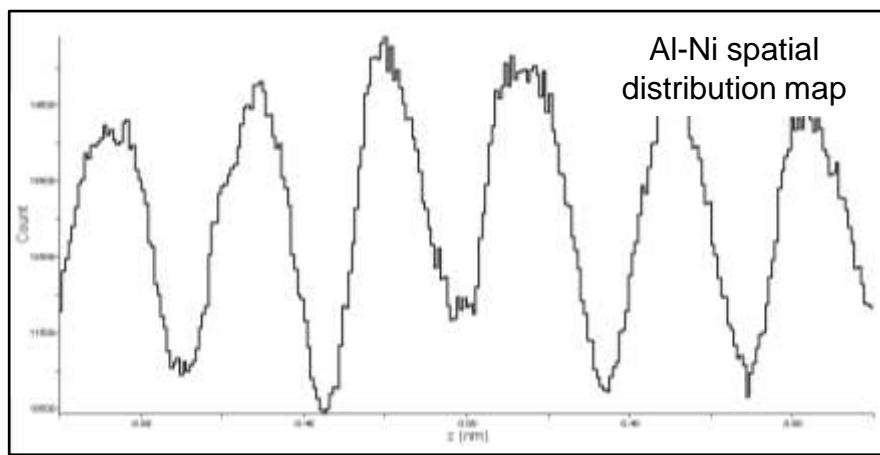
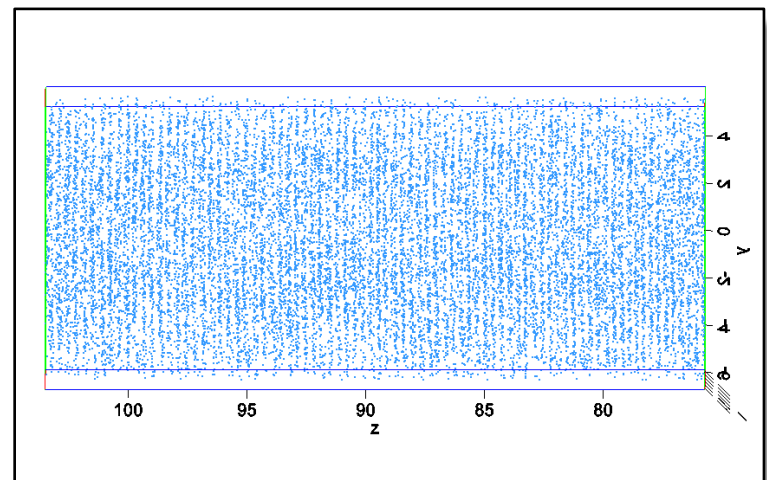
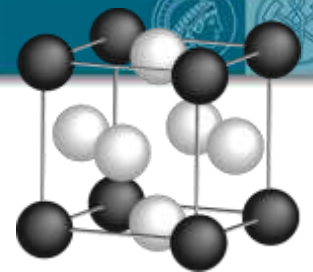
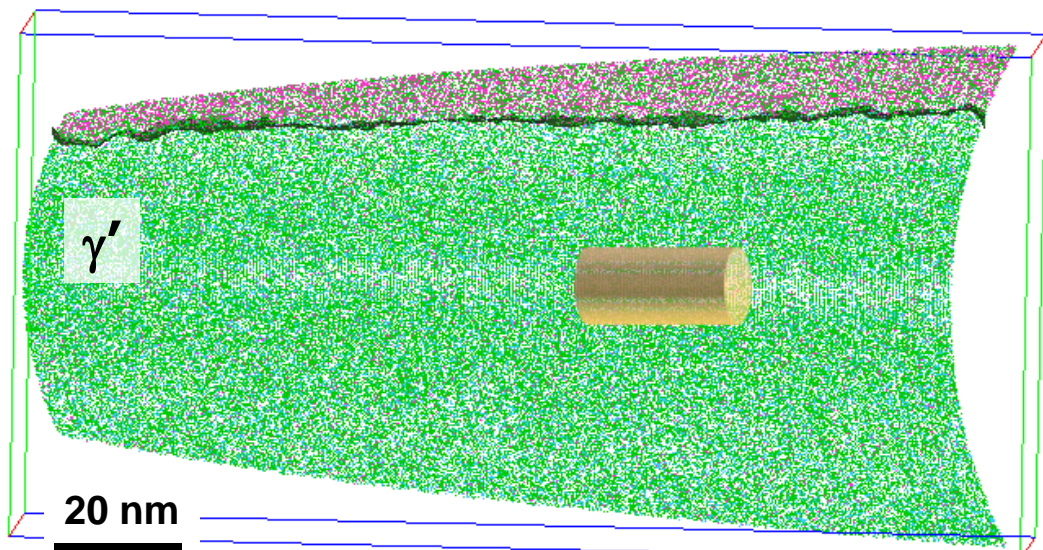
Field desorption image



Fe₃Al ordered phase (only Al displayed)



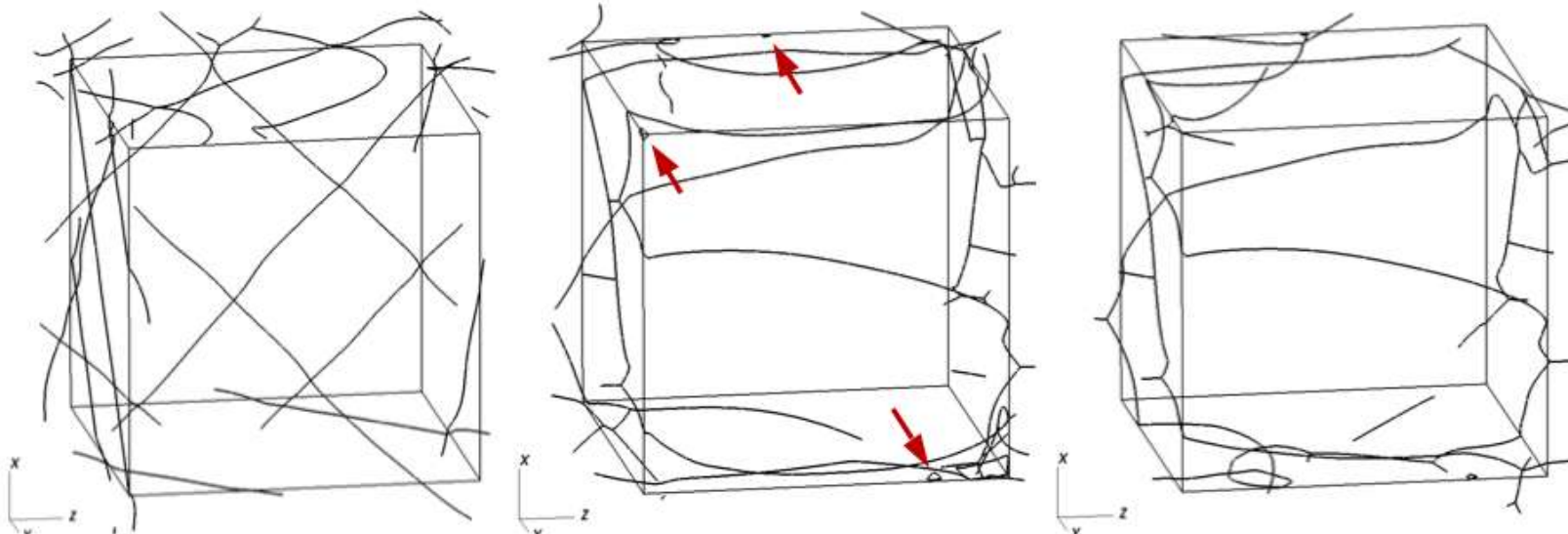
Lattice reconstruction



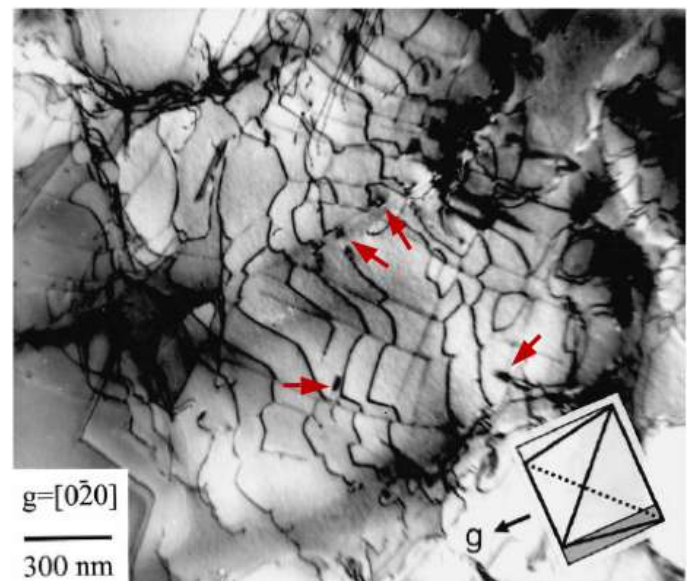
Lattice planes resolved:

- only in γ'
- only near (001) pole
- also in laser mode!

Microstructure at low stress creep

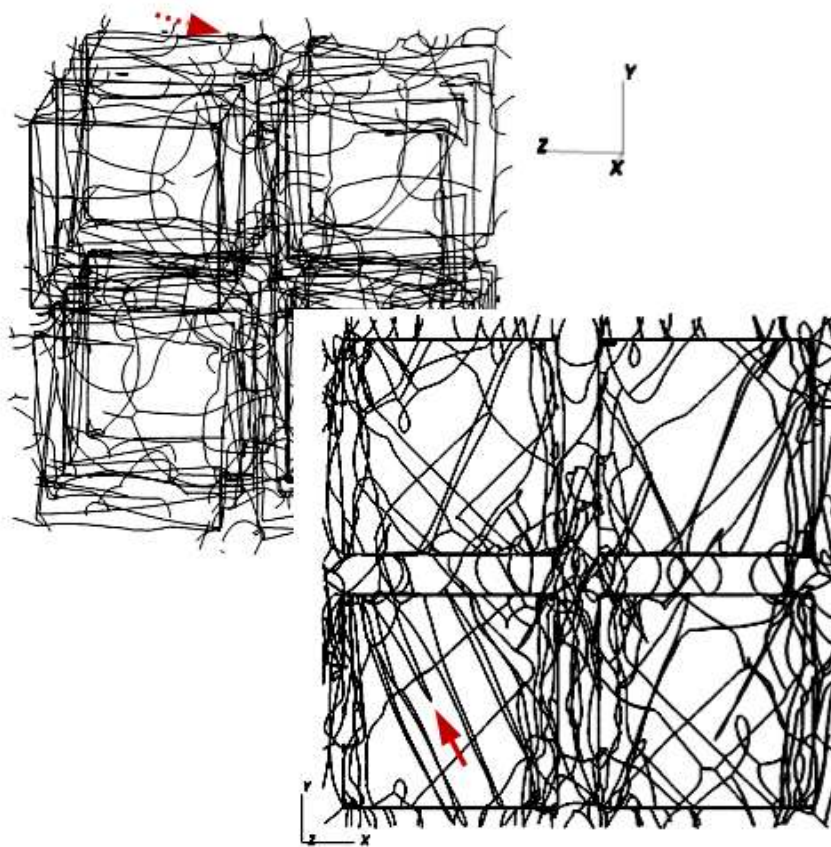


- Microstructure of the single crystal Ni base superalloy with loading conditions of 150 MPa with $Mg/Mc = 10$ at 0.0, 0.3 and 0.5 % creep strains.
- Experimental microstructure of Ni base superalloy in primary creep stage at 85 MPa shear loading condition.

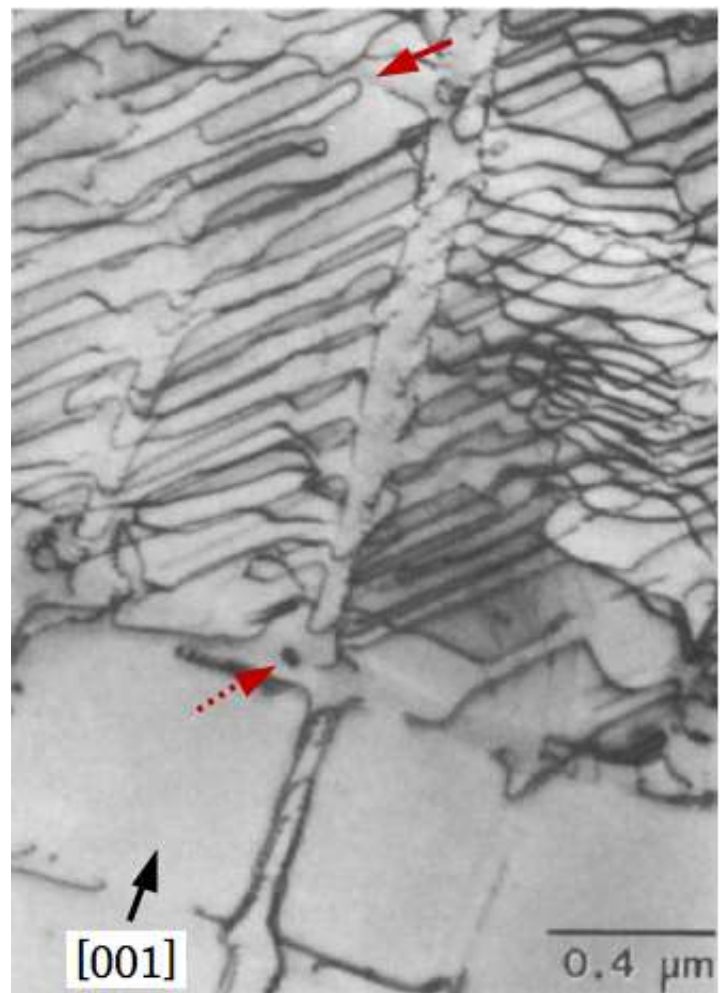


M. Kolbe, A. Dlouhy, G. Eggeler, Materials Science and Engineering A, 246 (1998) 133-142.

Microstructure at high stress creep

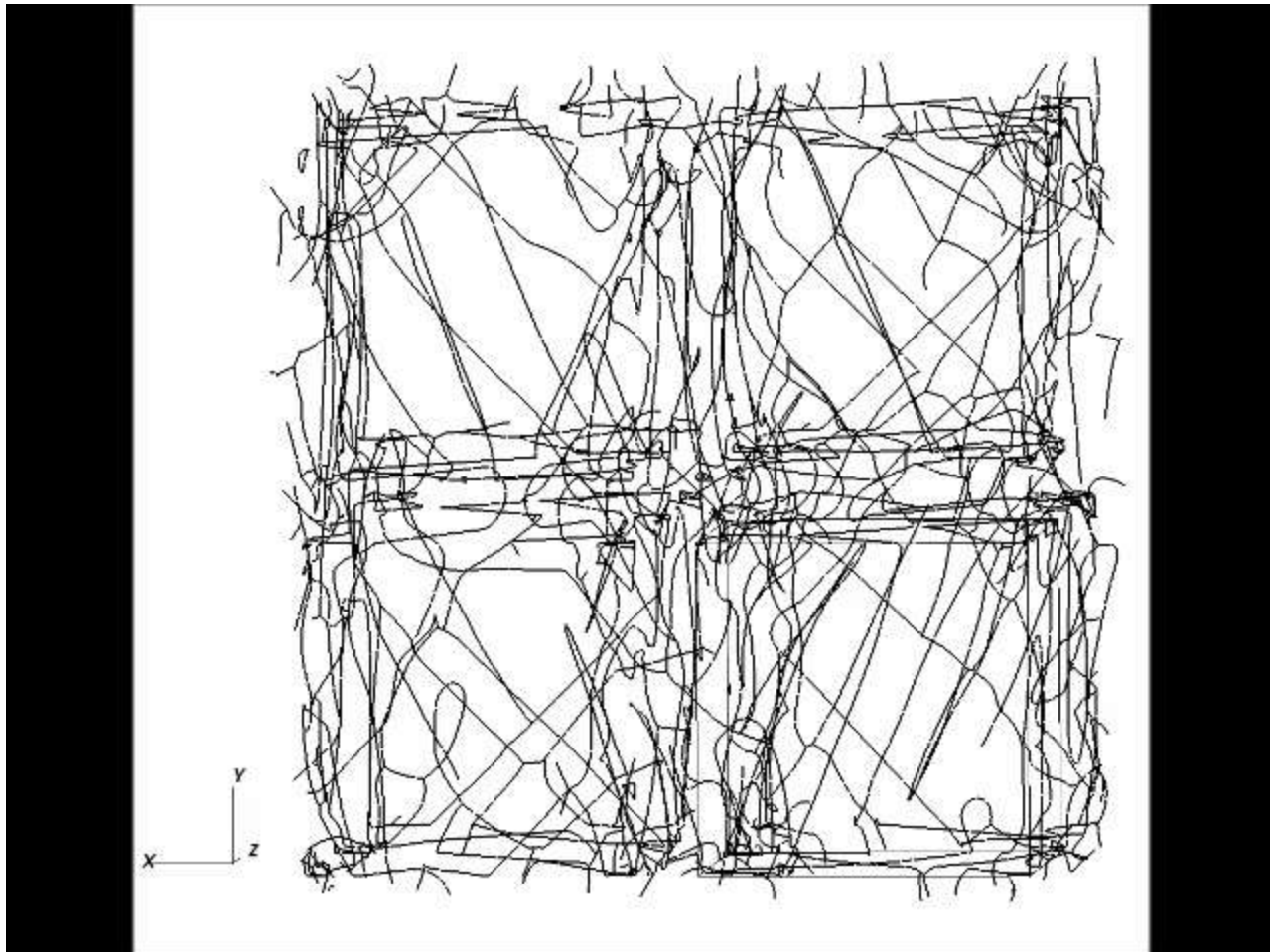


- 3D and 2D view of the DDD simulated creep microstructure of Ni base superalloy at 350 MPa loading along [100] with Mg/Mc = 10.
- Experimental creep microstructure of Ni base superalloy under 552 MPa loading along [001].

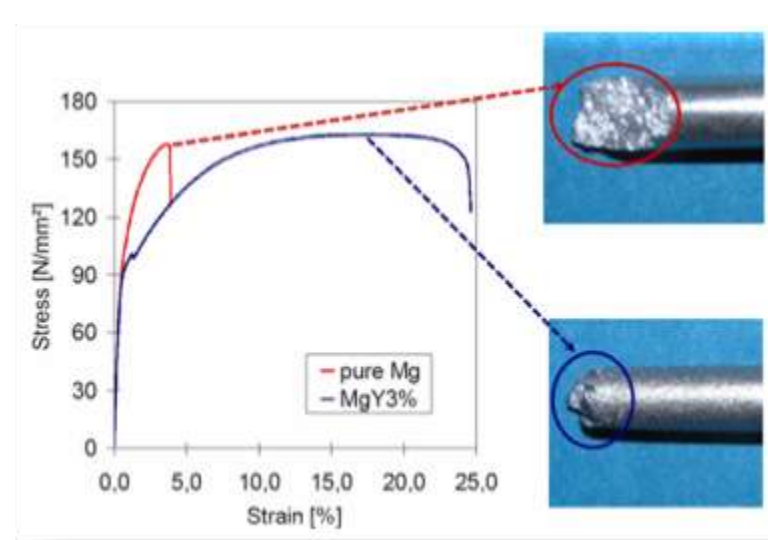
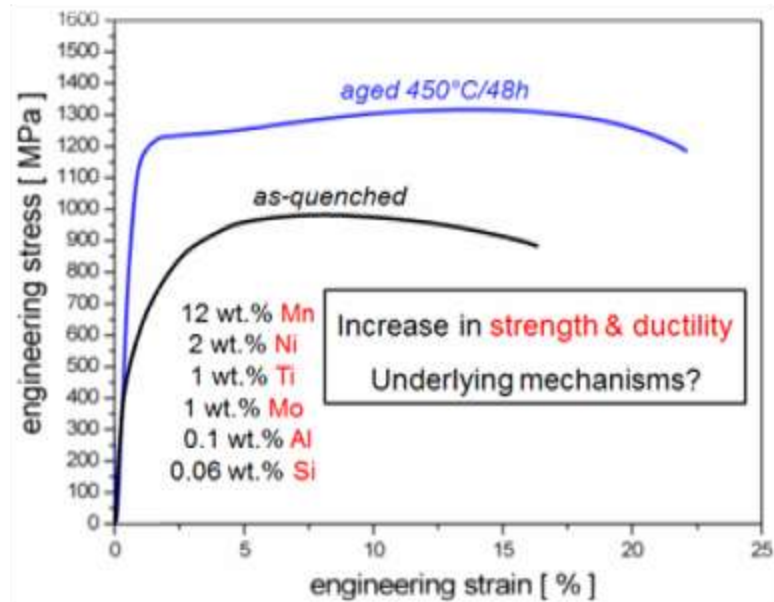
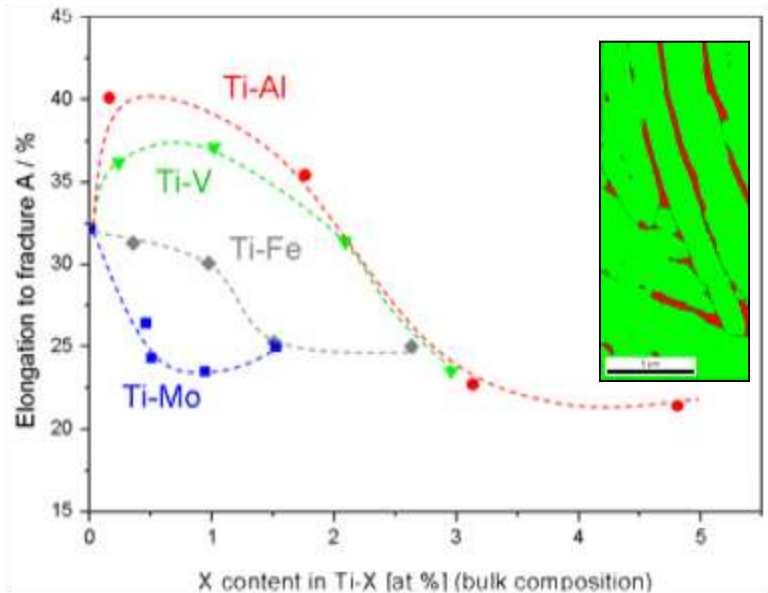


T.M. Pollock, A.S. Argon, Acta Metall Mater,
40 (1992) 1-30

Microstructure at high stress creep



Rapid alloy prototyping: other alloy systems





References

- O. Dmitrieva, D. Ponge, G. Inden, J. Millán, P. Choi, J. Sietsma, D. Raabe: *Acta Materialia* 59 (2011) 364-374, DOI: 10.1016/j.actamat.2010.09.042
Chemical gradients across phase boundaries between martensite and austenite in steel studied by atom probe tomography and simulation
- E.A. Marquis, P.-Pa Choi, F. Danoix, K. Kruska, S. Lozano-Perez, D. Ponge, D. Raabe, and C.A. Williams: *MICROSCOPY TODAY* 20(4) 44-48 (2012)
New Insights Into The Atomic-Scale Structures And Behavior Of Steels
- Y.J. Li, P. Choi, S. Goto, C. Borchers, D. Raabe, R. Kirchheim: *Acta Materialia*, Volume 60, Issue 9, May 2012, Pages 4005-4016
Evolution of strength and microstructure during annealing of heavily cold-drawn 6.3 GPa hypereutectoid pearlitic steel wire
- D. Raabe, P. P. Choi, Y.J. Li, A. Kostka, X. Sauvage, F. Lecouturier, K. Hono, R. Kirchheim, R. Pippan, D. Embury: *MRS Bulletin* 35 (2010) 982-991
Metallic composites processed via extreme deformation: Toward the limits of strength in bulk materials
- Y.J. Li, P.P. Choi, C. Borchers, S. Westerkamp, S. Goto, D. Raabe, R. Kirchheim: *Acta Materialia* 59 (2011) 3965–3977
Atomic-scale mechanisms of deformation-induced cementite decomposition in pearlite
- D. R. Steinmetz, T. Jäpel, B. Wietbrock, P. Eisenlohr, I. Gutierrez-Urrutia, A. Saeed-Akbari, T. Hickel, F. Roters, D. Raabe: *Acta Materialia* 61 (2013) 494-510
Revealing the strain-hardening behavior of twinning-induced plasticity steels: Theory, simulations, experiments
- F. Roters, P. Eisenlohr, L. Hantcherli, D.D. Tjahjanto, T.R. Bieler, D. Raabe: *Acta Materialia* 58 (2010) 1152–1211
Overview of constitutive laws, kinematics, homogenization and multiscale methods in crystal plasticity finite-element modeling: Theory, experiments, applications